Refractive Indexes of (Al, Ga, In)As Epilayers on InP for Optoelectronic Applications

M. J. Mondry, D. I. Babic, J. E. Bowers, and L. A. Coldren

Abstract—MBE grown bulk and short period superlattices of (Al,Ga,In)As epilayers lattice matched to InP were characterized by double-crystal diffractometry and low-temperature photoluminescence. A reflection spectroscopy technique was used to determine the refractive index of (Al,Ga,In)As films as a function of wavelength. The measured data were fitted to a single-oscillator dispersion model and the model coefficients are given. The resulting expression can be used in the design of waveguides, modulators, and other optical devices.

INTRODUCTION

(Al,Ga,In)As is an alternative material system to the InGaAsP system for optoelectronic applications based on InP substrates. The bandgap of the arsenide quaternary can be continuously varied from 1.47 eV ($Al_{0.48}In_{0.52}As$) to 0.75 eV ($Ga_{0.47}In_{0.53}As$) while maintaining a lattice constant matched to InP. The two ternary endpoints have a relatively large 0.5 eV conduction band offset, an attractive feature for electron confinement in quantum well structures. The material system also has the technological advantage of having only one Group V element, thus making composition control easier, especially in conventional molecular beam epitaxy (MBE) where the Group III elements can have near unity sticking coefficient under typical growth conditions. Excellent laser results using strained (Ga,In)As quantum wells [1] have been achieved, and low loss waveguides [2] have been demonstrated with (Al,Ga,In)As epilayers. The refractive index of (Al,Ga,In)As has been measured at certain wavelengths [3] and for specific multiquantum well structures [4]. However, little is known with regard to the index dispersion of (Al,Ga,In)As, an important material parameter for the design of any optoelectronic device.

This paper presents refractive index data of various (Al,Ga,In)As epilayers as a function of wavelength obtained by a reflection spectroscopy technique [4], [5]. This technique has the additional advantage that the wavelength dispersion of the refractive index can be determined. We also show that ternary superlattices of lattice-matched (Al,In)As and (Ga,In)As can be used to mimic high quality quaternary alloys. This has important implications in reducing the MBE growth complexity typically associated with quaternary alloys [6], i.e., grading of compositions or abrupt change of compositions.

MATERIALS GROWTH AND INDEX MEASUREMENT TECHNIQUE

The (Al,Ga,In)As epilayers were grown by conventional MBE (solid arsenic only) directly on InP substrates at substrate temperatures of 500° to 540°C measured with a pyrometer. The growth rate was kept fixed at 1 μm/h. The data of five samples used in this study are listed in Table I. Three of the samples (#3, #4, #5) were ternary short period superlattices of lattice-matched (Al,In)As and (Ga,In)As rather than homogeneous alloys. The superlattice epilayers were used to mimic the quaternaries as "digital" alloys because of the relative ease in which the effective composition can be controlled. Typically, composition changes are achieved by a mathematical modeling and computer control of the MBE sources to account for the time and setpoint responses in order to achieve the desired compositional profile [6]. The use of a "digital" alloy enables the composition to be controlled via the ratio of the (Al,In)As:(Ga,In)As layer thicknesses, which is a relatively simple task resulting in reduced growth complexity. We used a maximum layer thickness of 25 Å for either of the ternary layers.

The five samples in Table I correspond to three "effective" quaternary compositions X, formulated as $(Al_{0.48}In_{0.52}As)_X$ $(Ga_{0.47}In_{0.53}As)_{1-X}$. An endpoint ternary $Al_{0.48}In_{0.52}As$ epilayer (#1); a homogeneous alloy epilayer and superlattice epilayer (#2, #3) both having a quaternary fraction $X = 0.5$; and two superlattice epilayers (#4, #5) of two different periodicities both having quaternary fractions $X = 0.3$. The superlattice layer thicknesses were calculated from growth rates determined with RHEED oscillations. Alloy quality and composition was evaluated by a combination of double crystal X-ray diffraction and low temperature 1.4 K photoluminescence (PL). The quaternary model fraction X was determined by a linear interpolation [7] of the low temperature PL peak between the $Al_{0.48}In_{0.52}As$ ($E_g = 1.511$ eV [8]) and $Ga_{0.47}In_{0.53}As$ ($E_g = 0.800$ eV) endpoints. Despite the relatively large mismatch in superlattice samples #3 and #5, the PL FWHM is relatively narrow compared to published homogeneous quaternary data [7] indicating that the "digital" alloys are high optical quality material tolerant to lattice mismatch effects.

The refractive index of the epilayer was determined using a reflectance technique [5]. In this technique, a single epilayer of unknown refractive index is deposited on a substrate of known refractive index. The epilayer forms a Fabry–Perot etalon on top of the substrate yielding a reflection spectrum as shown in Fig. 1. The reflectivity spectra were measured using a Perkin–Elmer Lambda-9 spectrophotometer. Assum-
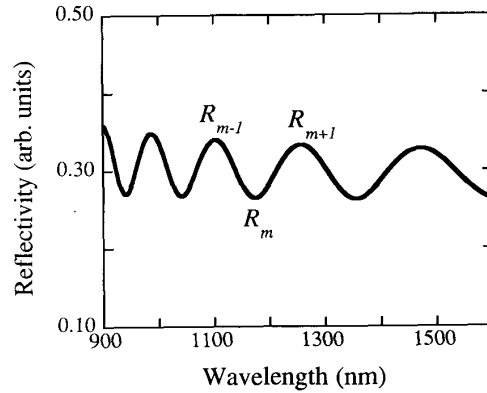
Fig. 1. Measured reflectance spectrum of an air/(Al,Ga,In)As/InP etalon structure. R_i designate the typical maximum-minimum extrema resulting from the Fabry–Perot effect.

TABLE I
MATERIAL ANALYSIS OF SAMPLES USED—Mole Fraction "X" defined as $(Al_{0.48}In_{0.52}As)_X(Ga_{0.47}In_{0.53}As)_{1-X}$

Sample #	Description	$\Delta a/a$	E_g@1.4K (eV)	P.L. FWHM (meV)	$Al_{0.48}In_{0.52}As$ Mole Fraction X
1	$Al_{0.48}In_{0.52}As$	3.3×10^{-4}	1.511	17.5	1.00
2	$Al_{0.24}Ga_{0.24}In_{0.52}As$	7.9×10^{-4}	1.140	7.3	0.48
3	(Al,In)As/(Ga,In)As 25 Å/25 Å	-2.7×10^{-3}	1.122	9.2	0.45
4	(Al,In)As/(Ga,In)As 6 Å/14 Å	-7.7×10^{-5}	1.016	6.5	0.30
5	(Al,In)As/(Ga,In)As 9 Å/24 Å	-1.2×10^{-3}	0.998	10.7	0.28

ing negligible loss in all materials, the amplitude of the reflectance fringes depends on the refractive indexes of the substrate n_s and the incident medium n_o, while the positions of the maxima and minima in the reflectivity spectrum depend only on its optical thickness. The extrema occur when the optical thickness equals an integral number of quarter-wavelengths:

$$n(\lambda_m)d = \frac{m\lambda_m}{4} \tag{1}$$

where $n(\lambda_m)$ is the epilayer refractive index at the position of extremum m, and d is the thickness of the epilayer. For even m, the structure reflectivity equals that of the air/substrate interface reflectivity, while for odd m, it equals that of a quarter-wavelength of epilayer. The refractive index of the epilayer is then given by

$$n(\lambda_m)^2 = n_o n_s \left(\frac{1 + r_s \sqrt{M_m}}{1 - r_s \sqrt{M_m}} \right) \tag{2}$$

where r_s is the amplitude reflectivity of the air/substrate interface and M_m is the *fringe amplitude*: the ratio of the local reflectivity maxima and minima. This ratio M_m is calculated at every extremum wavelength λ_m by interpolating between the two adjacent extrema, as shown in Fig. 1.

$$M_m = \left(\frac{R_{m-1} + R_{m+1}}{2R_m} \right)^{(-1)^m} . \tag{3}$$

In (2) and (3), we adopted the convention that $M_m > 1$ if $n(\lambda) > n_s$. The substrate refractive index dispersion causes the overall reflectivity spectrum to increase towards shorter wavelengths as shown in Fig. 1. This increases the measurement uncertainty in the fringe amplitude and mode position. We have minimized this error by performing the spectrophotometer background correction with a bare InP substrate (rather than a metal mirror). The fringe amplitude is the determined from a *normalized* reflectivity spectrum which oscillates around unity. The data of Pettit *et al.* [9] was used for the index dispersion of InP in the calculations.

The refractive index variation with frequency can be also determined using (1), given the knowledge of the exact epilayer thickness d and the mode numbers m. Unfortunately, the determination of the epilayer thickness to an accuracy better than $\pm 2\%$ is difficult by direct methods (e.g., profilometer or growth rate). Nevertheless, it is still possible to use the extrema positions to check the dispersion of the refractive index determined from (2). We compare the wavelength variation of the refractive index calculated from (1) and (2) by matching the index at the longest wavelength extrema point. Since the optical thickness of the epilayer has been made relatively small (~ 2 μm), the mode numbers ($m \sim 10$) can be unambiguously determined from the behavior of the optical path dispersion (Eq. (1)) and a second index dispersion curve is obtained. Comparison of the two curves confirmed that the two measurements are consistent. The presented formalism is no longer valid at the band edge due

to larger absorption. However, this limitation is minimal in the application to waveguide design since the region of interest is below the band edge (low loss).

RESULTS AND DISCUSSION

The index dispersion of the (Al,Ga,In)As quaternary for various (Al,In)As mole fractions, X, i.e., $(Al_{0.48}In_{0.52}As)_X$ $(Ga_{0.47}In_{0.53}As)_{1-X}$ is shown in Fig. 2. As can be seen, the ternary $Al_{0.48}In_{0.52}As$ ($X = 1.0$) has an index which is larger than that of InP, which is known from previous waveguide measurements [10]. For the $X = 0.5$ superlattice and homogeneous alloy epilayers, only a small difference in the index dispersion of the two samples is observed indicating that the "digital" and homogeneus alloys have a similar index dispersion below bandgap. The slight difference in the dispersion characteristics of the $X = 0.5$ samples can be attributed to the bandgap difference of the two samples, causing a 20 meV shift in their index dispersion. Unsurprisingly, the $X = 0.3$ superlattices with different periods display little difference in their dispersion properties, except for same bandgap shift as mentioned above.

Fitting the data to a first-order Sellmeier equation of the form

$$n(\lambda)^2 = A + \frac{B\lambda^2}{\lambda^2 - C^2} \tag{4}$$

we obtain the coefficients in Table II and plot these curve fits on Fig. 2. The curve fits given by the coefficients in Table II have a maximum rms deviation of $< 4 \times 10^{-3}$ from the measured data. We have also empirically fitted the A, B, and C coefficients as a function of $Al_{0.48}In_{0.52}As$ composition X given as

$$A(X) = 9.689 - 1.012X$$
$$B(X) = 1.590 - 0.376X$$
$$C(X) = 1102.4 - 702.0X + 330.4X^2 \tag{5}$$

where $0.3 < X < 1.0$. Though the curve fits generated by the coefficients in (5) are less accurate, having a maximum rms deviation of $< 7 \times 10^{-3}$ from the measured data, they yield an analytical expression for the index dispersion as a function of composition, useful for device design purposes.

For comparison, the index data from De Bernardi *et al.* [3] measured using a waveguide cutoff method is also shown in Fig. 2. As can be seen in the Figure, the refractive index values from their measurement are all slightly greater than corresponding values from our fitted curves. These discrepancies, however, can be accounted for in part by the difference in the InP refractive index used in the index calculations, since both measurements yield only *the refractive index difference relative to the substrate or cladding epilayer*. The other contribution to the differences in the data is the error in the measurement techniques itself. Empirically, we have found that we can reproduce these index dispersion curves from a given sample to within $\Delta n < 5 \times 10^{-3}$. Thus, our data and De Bernardi *et al.* correlate within this combined range of calculation and measurement uncertainty.

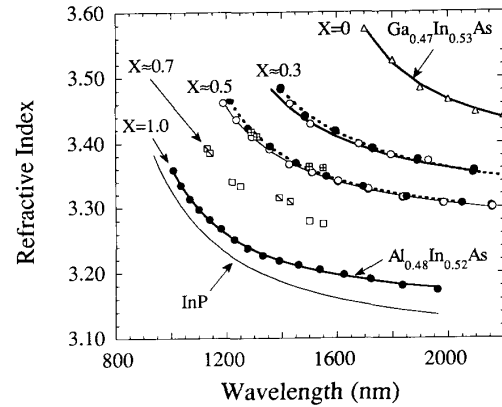In conclusion, we have measured the index dispersion of

Fig. 2. Refractive index of $(Al_{0.48}In_{0.52}As)_X(Ga_{0.47}In_{0.53}As)_{1-X}$ as function of wavelength for several (Al,In)As mole fractions "X". The data indicated by closed and open circles is this work. The open and patterned squares are data from De Bernardi *et al.* [3]. The solid and dashed curves from top to bottom are: $Ga_{0.47}In_{0.53}As$ from [5], our curve fits using the coefficients in Table II, and InP from [8].

TABLE II
COEFFICIENTS FOR CURVE FITS SHOWN IN FIG. 2

Mole Fraction X	A	B	C (nm)
1.00	8.650	1.239	730.8
0.48	9.320	1.322	844.2
0.45	9.615	1.056	905.9
0.30	9.481	1.423	925.9
0.28	9.255	1.599	928.3

three different compositions of (Al,Ga,In)As grown on InP by a reflectance technique. We have shown that a short period superlattice of (Al,In)As/(Ga,In)As can be used as a high-quality substitute for the homogeneous quaternary alloy. Fitting the data to a single oscillator model, we obtained analytical expressions accurate to within to 5×10^{-3} which are useful in the design of (Al,Ga,In)As optoelectronic devices.

REFERENCES

[1] A. Kasukawa, R. Bhat, C. E. Zah, M. A. Koxa, S. A. Schwarz, and T. P. Lee, "200 A/cm^2 threshold current density 1.5 μm GaInAs/AlGaInAs strained-layer GRIN-SCH quantum well laser diodes grown by OMCVD," presented at Device Res. Conf., Boulder, CO, IIA-2, June 1991.

[2] P. Cinguino, F. Genova, S, Morasca, C. Rigo, and A. Stano, "Low-loss ridge optical waveguides in quaternary InGaAlAs/InP grown by MBE," *Electron. Lett.*, vol. 23, pp. 235–236, Feb. 26, 1987.

[3] C. Be Bernardi, M. Meliga, S. Morasca, C. Rigo, B. Sordo, and A. Stano, "Refractive indices of InGaAlAs grown by molecular beam epitaxy," *J. Apply. Phys.*, vol. 68, pp. 6513–6514, Dec. 15, 1990.

[4] S. Nojima and H. Asahi, "Refractive index of InGaAs/InAlAs multi-quantum-well layers grown by molecular-beam epitaxy," *J. Appl. Phys.*, vol. 63, pp. 479–483, Jan. 15, 1988.

[5] P. Chandra, L. A. Coldren, and K. E. Strege, "Refractive index data from $Ga_xIn_{1-x}As_yP_{1-y}$ films," *Electron. Lett.*, vol. 17, pp. 6–7, Jan. 8, 1981.

[6] J. C. Vlcek and C. G. Fonstad, "Precise computer control of the

MBE process-application to graded InGaAlAs/InP alloys,'' *J. Crystal Growth*, vol. 111, pp. 56–60, May 1991.

[7] J. P. Praseuth, M. C. Joncour, J. M. Gérard, P. Hénoc, and M. Quillec, "Growth and characterization of AlGaInAs lattice matched to InP grown by molecular-beam epitaxy," *J. Appl. Phys.*, vol. 63, pp. 400–403, Jan. 15, 1988.

[8] D. Oertel, D. Bimberg, R. K. Bauer, and K. W. Carey, "High-precision band-gap determination of $Al_{0.48}In_{0.52}As$ with optical and structural methods," *J. Appl. Phys.*, vol. 55, pp. 140–141, July 10, 1989.

[9] G. D. Pettit and W. J. Turner, "Refractive index of InP," *J. Appl. Phys.*, vol. 36, p. 2081, 1965.

[10] S. Ritchie, E. G. Scott, and P. M. Rodgers, "Optical waveguides in $In_{0.52}Al_{0.48}As$ grown on InP by MBE," *Electron Lett.*, vol. 22, pp. 1066–1068, Sept. 25, 1986.

High Silica Waveguides on Alumina Substrates for Hybrid Optoelectronic Integration

C. J. Sun, W. M. Myers, K. M. Schmidt, S. Sumida, and K. P. Jackson

Abstract—High silica optical waveguides are fabricated on alumina substrates by flame hydrolysis deposition (FHD) and reactive ion etching (RIE) patterning techniques. The composition of the high silica glass waveguides is adjusted from that of the conventional FHD glass to reduce the thermal expansion mismatch between silica glass and alumina. Thus made glass waveguides exhibit low loss and are compatible with various types of alumina ceramic substrates.

Introduction

OPTICAL interconnects are potentially advantageous over their electrical counterparts for many high-speed computer processing and networked computer systems [1]–[3]. Critical to the success of implementing these interconnections in this high-performance computing environment is the optical packaging of the associated optoelectronic (O-E) components and optical fibers. Dense, compact, high-speed O-E modules and optical interfaces must be assembled using processes and materials that are compatible with high performance electronic packaging. Planar-processed optical waveguides acting as interfaces between O-E components and optical fibers may play a major role in optical packaging. Optical waveguides can allow higher packing density of optoelectronic components (e.g., fan-in/fan-out from fiber to arrays of O-E devices) and greater flexibility in component placement (e.g., eliminating edge-mounted components and/or fiber pigtails). They also provide integrated optical circuit elements that process optical signals or facilitate O-E coupling (e.g., [4], [5]).

A significant amount of work has been carried out on

different optical waveguide materials and devices and the emphasis is shifting towards manufacturability and the compatibility of these optical waveguides with electronic packaging techniques [6]. High silica glass waveguides fabricated by flame hydrolysis deposition and reactive ion etching have been used to realize a wide variety of integrated optical devices on quartz and silicon substrates [7]. This technology is attractive for the packaging of O-E components and optical fibers because of its process maturity and material compatibility with subsequent electronic packaging processes such as high-temperature chip attach soldering. In this letter, we describe the fabrication and optical quality of these high silica glass waveguides formed on ceramic substrates containing 99% alumina for electronic thin-film applications and 96% and 92% alumina for thick-film applications by using the same technology. Alumina is a common electronic packaging substrate for use in hybrid microwave circuitry and is also being considered for hybrid optoelectronic packaging [8].

Waveguide Fabrication

Flame hydrolysis deposition was applied to form two layers of silica glass films on IBM 92% and commercially available 99% and 96% alumina substrates. Both layers were doped with GeO_2, B_2O_3, and P_2O_5. The top layer was the waveguide core with higher refractive index. The refractive index was adjusted by the GeO_2 content. Both singlemode and multimode planar waveguides have been fabricated; however, the following discussion will focus on multimode waveguides with 0.2 numerical aperture (NA), i.e., 1% refractive index difference. The core thickness was from 10 to 50 μm and the cladding was around 50 to 60 μm thick. An application for this waveguide is discussed in [9].

Because of the large thermal expansion difference between silica glass and alumina, the stress of high silica glass film deposited on alumina is much higher than that of silica formed on silicon substrates. Fig. 1 shows the estimated film